Insights into the Structural Basis of N2 and O6 Substituted Guanine Derivatives as Cyclin-Dependent Kinase 2 (CDK2) Inhibitors: Prediction of the Binding Modes and Potency of the inhibitors by Docking and ONIOM Calculations

Jans H. Alzate-Morales,* Julio Caballero, Ariela Vergara Jague, and Fernando D. González Nilo

Centro de Bioinformática y Simulación Molecular, Universidad de Talca, 2 Norte 685,
Casilla 721, Talca, Chile

N2 and O6 substituted guanine derivatives are well-known as potent and selective CDK2 inhibitors. The ability of molecular docking using the program AutoDock3 and the hybrid method ONIOM, to obtain some quantum chemical descriptors with the aim to successfully rank these inhibitors, was assessed. The quantum chemical descriptors were used to explain the affinity, of the series studied, by a model of the CDK2 binding site. The initial structures were obtained from docking studies and the ONIOM method was applied with only a single point energy calculation on the protein−ligand structure. We obtained a good correlation model between the ONIOM derived quantum chemical descriptor "H-bond interaction energy" and the experimental biological activity, with a correlation coefficient value of R = 0.80 for 75 compounds. To the best of our knowledge, this is the first time that both methodologies are used in conjunction in order to obtain a correlation model. The model suggests that electrostatic interactions are the principal driving force in this protein−ligand interaction. Overall, the approach was successful for the cases considered, and it suggests that could be useful for the design of inhibitors in the lead optimization phase of drug discovery.

INTRODUCTION

The cyclin dependent kinases (CDKs) are a class of enzymes which play a fundamental role in cell cycle regulation.[1,2] Particularly, as their name suggest, CDKs activation partially depends on the binding of other class of proteins named cyclins. For example cyclins of the D family complex with CDK4 and CDK6 during G1 phase, cyclin E with CDK2 in late G1, cyclin A with CDK2 in S phase, and cyclin B with CDK1 (also known as cdc2) in late G2/M. Then, aberrant CDK control and consequent loss of cell cycle checkpoint function have been directly linked to the molecular pathology of cancer.[3] It is well-known that phosphorylation in a conserved threonine residue of the CDK subunit is required for its complete activation. This task is performed by the CDK activating kinase. These proteins properly regulate the cell cycle progress and DNA synthesis only as an active complex (T160pCDK/cyclin).[4] Overall, the activity of the CDK/cyclin complex can be depleted by at least two different mechanisms: the phosphorylation of the CDK subunit at the inhibitory sites or the binding of the specialized natural inhibitors known as CDK inhibitors. In the first mechanism, the amino acid residue Y15 and to a lesser extend T14 (in CDK2) are phosphorylated by human Wee 1 Hu.[5] This inhibitory phosphorylation is independent of previous cyclin binding.[6] The second mechanism involves the binding of natural CDK inhibitors. Four major mammalian CDK inhibitors have been discovered. P21 (CIP1/WAF1) and p27 (KIP1) inactivate CDK2 and CDK4 cyclin complexes by binding to them. P16$_{INK4}$ and p15$_{INK4B}$ are specific for CDK4 and CDK6. They inhibit the formation of the active cyclin complexes by binding to the inactive CDK, and they can also bind to the active complex.[7,2] However, it has been shown that natural CDK inhibitors are subexpressed in some carcinogenic cells, and medicinal chemists have put some of their effort in the search for new synthetic inhibitors to replace them.[8−12] Some of them have entered in clinical trials, for instance flavopiridol was the first potent inhibitor of cyclin-dependent kinases to reach clinical trial. In the majority of solid tumor cell lines and xenografts, flavopiridol induces cell cycle arrest and tumor growth inhibition.[13]

The search for more potent and selective CDK inhibitors is a daunting challenge due to the similarity of the ATP binding site along the different CDK subtypes.[14] According to this, the development and use of new strategies to overcome this problem are urgently needed. Nowadays, new and exciting strategies have emerged and become available to find more potent and selective inhibitors, and they normally use structure−activity relationships (SAR) derived from different computational calculation approaches.[15−19]

In previous studies, we have developed some computational protocols with the aim to classify a smaller set of CDK2 inhibitors belonging to the same family of compounds studied here. For instance, we applied the hybrid quantum mechanics/molecular mechanics (QM/MM) method to determine the protein−ligand interaction energy between CDK2 and five inhibitors with the N^2-substituted 6-cyclohexyl-methoxypurine scaffold. The computational results in that work showed that the QM/MM interaction energy was strongly correlated to the biological activity and can be used as a predictor, at least within a family of substrates.[20] However, the set of compounds studied was very small, and

* Corresponding author phone: 56-71-201 685; fax: 56-71 201 662; e-mail: jalzate@utalca.cl or jalzatemorales@gmail.com.

the computational resources to obtain the interaction energy from QM/MM scheme were expensive. In a second computational approach, we reported a theoretical study on a more extended set of CDK2 inhibitors (16 compounds) using a set of global reactivity indices defined in terms of the density of states within the framework of density functional theory (DFT). The comparison between the biological activity and the electronic chemical potential approached as the Fermi level yielded poor results, thereby suggesting that the interaction between the hinge region (HR) of CDK2 and the ligands may have a marginal contribution from the charge transfer (CT) component. Comparison between the biological activity and global softness showed a better correlation, thereby suggesting that polarization effects outweigh CT contribution in the HR-ligand interaction.[21] Despite the insight gained in those previous studies, they lacked of a representative and statistical meaningful set of inhibitors, and the computational methodologies used were expensive. The present study wants to surpass these problems and go beyond in the searching for new computational and easy to obtain descriptors for rank the set of CDK2 inhibitors studied here.

According to this, we present a computational study which combines two powerful computational strategies: docking and ONIOM (Our own N-layered Integrated molecular Orbital and Molecular Mechanics), with the aim to establish some useful SAR for the CDK2 inhibition by N2 and O6 substituted guanine derivatives (see Table 1).[22−24] The software AutoDock3[25] was used to obtain the best pose for each inhibitor structure within the CDK2 binding site. The best inhibitor structure was selected according to its docked free energy value and its position within the binding site. Once the best structure was selected, ONIOM method was applied for deriving quantum chemical descriptors. A relationship was established between the CDK2 inhibitor's experimental activities and some of these descriptors.

METHODOLOGY AND COMPUTATIONAL DETAILS

Data Used in Analysis. The *in vitro* biological activity data reported as IC_{50} values in recent literature for inhibition produced by N2 and O6 substituted guanine derivatives on the T160pCDK2/cyclinA enzymatic system were used. All compounds were obtained from previous articles reported by the same research group.[22−24] The whole data set included 80 compounds, which biological activity (IC_{50} values) was determined for inhibition of CDK2 (see Table 1). Those molecules which did not have biological activity, for inhibition of the enzyme under study, in exact numerical form were excluded from the analysis. For modeling, IC_{50} values were converted into logarithmic activities $\log (10^6/IC_{50})$, where 10^6 guarantees that logarithmic activities range between 1 and 9. It is worthy to say that IC_{50} values span a broad range from 0.0054 to 90 μM.

Docking Studies. In molecular docking, we attempt to predict the structure (or structures) of the intermolecular complex formed between two or more molecules. Docking is widely used to suggest the binding modes of protein inhibitors. Most docking algorithms are able to generate a large number of possible structures, and so they also require a means to score each structure to identify those of most interest. In general, the "docking problem" is thus concerned with the generation and evaluation of plausible structures of intermolecular complexes.[26,27]
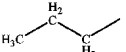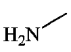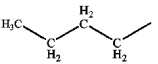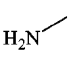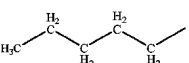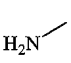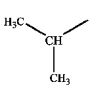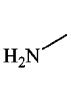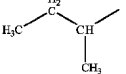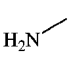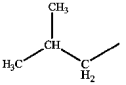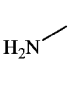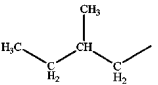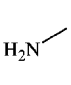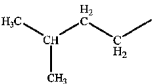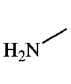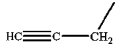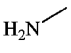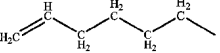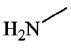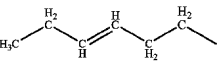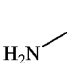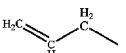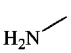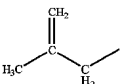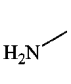
The first step in our study was the validation of docking methodology on the modeled system. 3D structures of compounds **29**, **34**, **28**, **27**, **48**, **47**, **40**, and **65** were extracted from the cocrystallized complex with T160pCDK2/Cyclin A (PDB codes: 1H1S, 1H1R, 1H1Q, 1H1P, 1OIY, 1OIU, 1OI9, and 2G9X, respectively) and were further geometrically optimized using the semiempirical quantum chemical method AM1[28] implemented in the MOPAC 6.0 computer software package.[29] Partial Mulliken atomic charges were computed, using MOPAC and applying the AM1 Hamiltonian, in an ORIGIN300 computer with 8 processors R1400 and 8GB RAM. The structure optimization and partial atomic charges calculations were run in a single processor.
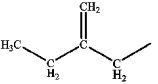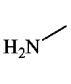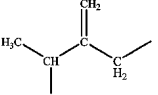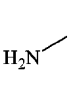
The protein structures were visualized and built with the software Insight II.[30] All water molecules were removed from the protein structure, and polar hydrogen atoms were added assuming a physiological pH value of 7.0. The CVFF[31] force field was used to assign the partial atomic charges to the protein. After that, docking of the eight inhibitors mentioned above into the binding pocket of CDK2 was carried out using the AutoDock3[25] program. The protein and ligand structures were opened and prepared with the AUTODOCKTOOLS version 1.4.4.[32] Nonpolar hydrogen atoms were merged, for the ligand structures, within the united atom approach using the program AUTOTORS, which is part of the AutoDock3 program package. This program also defines which bonds are allowed to rotate freely during the automated docking process, and it saves the ligands in the PDBQ format. All rotatable ligand bonds defined by default for the program were allowed to rotate during the automated docking process. The solvation parameters were added, and the prepared protein structures were saved in the pdbqs-format suitable for calculating energy grid maps using the program AUTO-GRID. A grid size of 70 × 70 × 70 points with a spacing of 0.375 Å was applied, which corresponds to a cube with an edge length of 26.3 Å. The center of the grid box was defined as the center of the cocrystallized inhibitor.

Docking calculations were performed with a maximum number of 300 optimization steps in the local search. For the docking runs employing the standard optimization algorithms incorporated in AutoDock3, the population size was set to 100 individuals and iterated through 1.000.000 energy evaluations. Other parameters were set to their default values.

Once the docking protocol described above was validated, that means the position and orientation taken by the ligands in some of the most representative X-ray structures of the system T160pCDK2/cyclinA available in the Protein Data Bank (PDB)[33] were reproduced with good accuracy; the remaining compounds were optimized and docked following the same protocol. The protein crystal structure of the most active CDK2 inhibitor (**29**) (PDB code: 1H1S) was chosen to perform the remaining docking studies. This choice was based on two important facts: a) the fully active conformation of CDK2 which is important to represent all conformational changes experimented by the protein after binding of cyclin A and phosphorilation in residue Thr160 and b) the cocrystalized structure with compound **29** (Nu6102), the most potent compound in the series studied. One can assume that main interactions satisfied by the most active compound in

Table 1. CDK2 Inhibitor Structures, IC$_{50}$ (μM) Values, and ONIOM Component Energies for the Set of Compounds Studied

Compd	R1	R2	CDK2 inhibition (IC$_{50}$ (μM))	ΔE^{ONIOM}	ΔE^{ONIOM} (High, A)	ΔE^{ONIOM} (Mid, AB-A)	ΔE^{ONIOM} (Low, ABC-AB)
1		H$_2$N	67 ± 5	-14.92	-13.67	-0.16	-1.09
2		H$_2$N	48 ± 7	-16.93	-15.59	-0.09	-1.25
3		H$_2$N	49 ± 7	-17.64	-16.49	-0.12	-1.03
4		H$_2$N	75 ± 10	-17.31	-18.09	-0.01	0.80
5		H$_2$N	25 ± 1	-17.81	-17.56	0.00	-0.26
6		H$_2$N	42 ± 5	-14.15	-14.09	-0.10	0.04
7		H$_2$N	15 ± 2	-12.21	-15.07	-0.04	2.89
8		H$_2$N	26 ± 9	-17.65	-16.85	-0.10	-0.70
9		H$_2$N	90 ± 7	ND	ND	ND	ND
10		H$_2$N	47 ± 4	-18.27	-17.42	-0.32	-0.53
11		H$_2$N	69 ± 8	-22.60	-18.05	-0.03	-4.52
12		H$_2$N	78 ± 13	ND	ND	ND	ND
13		H$_2$N	35 ± 6	-14.90	-17.14	0.14	2.11
14		H$_2$N	21 ± 2	-16.86	-14.70	-0.04	-2.12
15		H$_2$N	16 ± 1	-10.82	-14.21	-0.01	3.40

Table 1. Continued
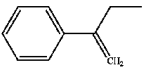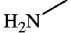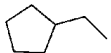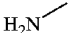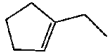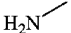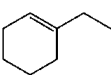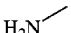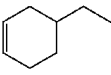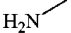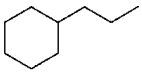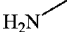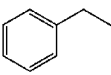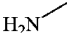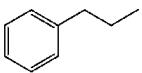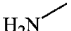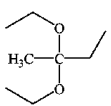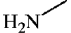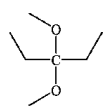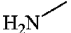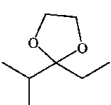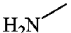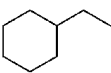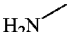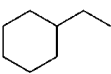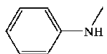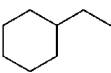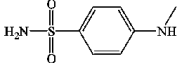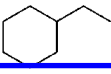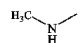
Compd	R1	R2	CDK2 inhibition (IC$_{50}$ (μM))	ΔE^{ONIOM}	ΔE^{ONIOM} (High, A)	ΔE^{ONIOM} (Mid, AB-A)	ΔE^{ONIOM} (Low, ABC-AB)
		Substituents		ONIOM energy components (kcal/mol)			
16			34 ± 3	-20.29	-16.19	-0.39	-3.71
17			21 ± 3	-14.12	-15.99	-0.06	1.93
18			31 ± 7	-16.92	-18.05	-0.08	1.21
19			22 ± 4	-17.92	-17.50	-0.04	-0.37
20			16	-4.33	-15.22	-0.10	11.00
21			44 ± 3	-14.95	-12.61	-0.23	-2.11
22			35 ± 6	-17.58	-16.41	-0.14	-1.04
23			65 ± 6	-7.85	-11.68	0.01	3.83
24			33 ± 6	-24.73	-18.40	-1.08	-5.25
25			20 ± 5	-18.69	-18.74	0.00	0.05
26			65 ± 2	-18.69	-17.76	0.36	-1.29
27 (NU2058)			17 ± 2	-13.01	-13.50	-0.15	0.63
28 (NU6094)			0.97 ± 00.3	-13.95	-17.38	-0.01	3.44
29 (NU6102)			0.0054 ± 0.001	-30.39	-43.32	-0.29	13.22
30			5.0 ± 0.3	-30.50	-19.49	-2.64	-8.37

Table 1. Continued
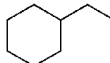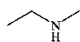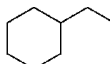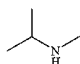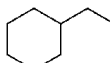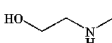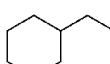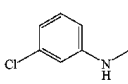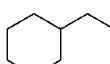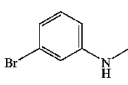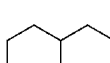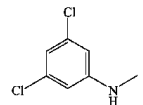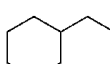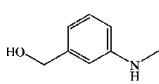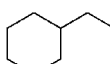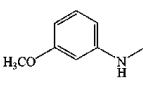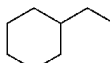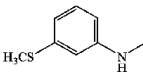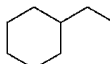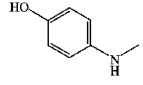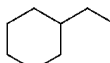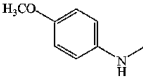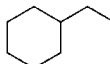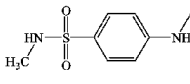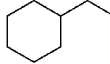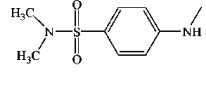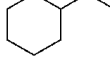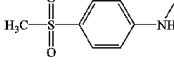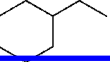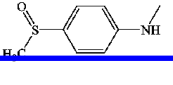
Compd	R1	R2	CDK2 inhibition (IC$_{50}$ (µM))	ΔE^{ONIOM}	ΔE^{ONIOM} (High, A)	ΔE^{ONIOM} (Mid, AB-A)	ΔE^{ONIOM} (Low, ABC-AB)
31	cyclohexyl-ethyl	ethyl-NH-methyl	2.8 ± 0.4	-18.10	-16.44	-0.33	-1.32
32	cyclohexyl-ethyl	isopropyl-NH-methyl	1.2 ± 0.2	-14.91	-15.09	-0.41	0.58
33	cyclohexyl-ethyl	HO-ethyl-NH-methyl	2.8 ± 0.9	-20.34	-21.13	-0.42	1.21
34 (NU6086)	cyclohexyl-ethyl	Cl-phenyl-NH-methyl	2.3 ± 0.3	-12.50	-18.91	-0.63	7.04
35	cyclohexyl-ethyl	Br-phenyl-NH-methyl	6.8 ± 4.8	-21.93	-20.79	-0.07	-1.07
36	cyclohexyl-ethyl	Cl,Cl-phenyl-NH-methyl	12 ± 6	-10.19	-16.02	-0.38	6.21
37	cyclohexyl-ethyl	HO-CH$_2$-phenyl-NH-methyl	0.4 ± 0.1	-9.45	-22.81	-0.04	13.39
38	cyclohexyl-ethyl	H$_3$CO-phenyl-NH-methyl	1.8 ± 0.2	-18.54	-21.59	-0.76	3.81
39	cyclohexyl-ethyl	H$_3$CS-phenyl-NH-methyl	1.7 ± 0.1	-22.52	-23.51	-0.74	1.73
40	cyclohexyl-ethyl	HO-phenyl-NH-methyl	0.069 ± 0.001	-20.42	-23.48	-0.08	3.14
41	cyclohexyl-ethyl	H$_3$CO-phenyl-NH-methyl	0.65 ± 0.03	-15.30	-15.09	-0.05	-0.16
42	cyclohexyl-ethyl	H$_3$C-NH-SO$_2$-phenyl-NH	0.007 ± 0.0001	-18.79	-38.63	-1.11	20.95
43	cyclohexyl-ethyl	(H$_3$C)$_2$N-SO$_2$-phenyl-NH	0.056 ± 0.020	-23.05	-31.88	-0.37	9.20
44	cyclohexyl-ethyl	H$_3$C-SO$_2$-phenyl-NH	0.063 ± 0.007	-27.19	-35.26	-0.55	8.62
45	cyclohexyl-ethyl	H$_3$C-SO-phenyl-NH	0.10 ± 0.01	-19.24	-31.97	-0.68	13.40

Table 1. Continued

Compd	R1	R2	CDK2 inhibition (IC$_{50}$ (μM))	ΔE^{ONIOM}	ΔE^{ONIOM} (High A)	ΔE^{ONIOM} (Mid, AB-A)	ΔE^{ONIOM} (Low, ABC-AB)
		Substituents		ONIOM energy components (kcal/mol)			
46			0.070 ± 0.008	NI	NI	NI	NI
47			0.21 ± 0.04	-21.05	-27.73	-0.29	6.97
48			0.064 ± 0.033	-22.39	-32.29	-1.45	11.34
49			0.20 ± 0.03	-2.96	-27.78	-0.55	25.37
50			0.20 ± 0.04	2.56	-27.31	-0.71	30.59
51			0.30 ± 0.04	-24.55	-27.89	-0.35	3.69
52			0.8 ± 0.2	NI	NI	NI	NI
53			0.13 ± 0.02	NI	NI	NI	NI
54			0.30 ± 0.03	-20.18	-35.36	-0.37	15.55
55			1.7 ± 0.9	-14.76	-17.48	-0.17	2.90
56			5.0 ± 0.2	-9.93	-26.76	-0.46	17.29
57			4.3 ± 1.1	-13.26	-20.36	-0.03	7.13

Table 1. Continued
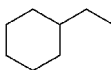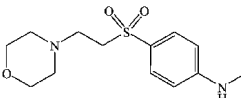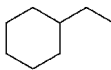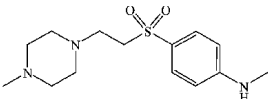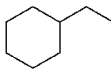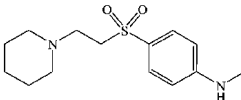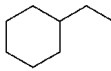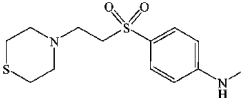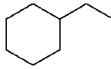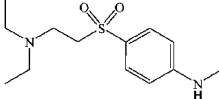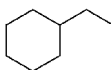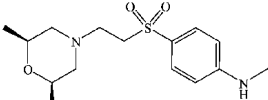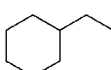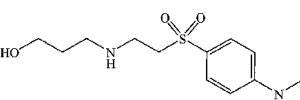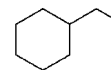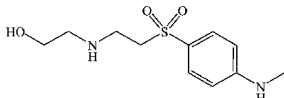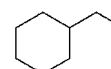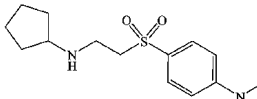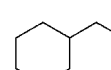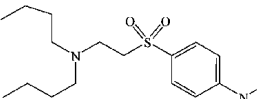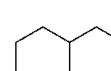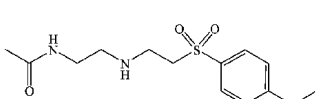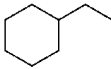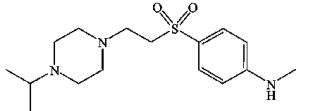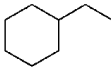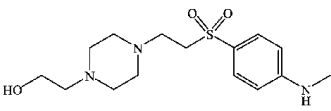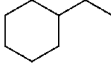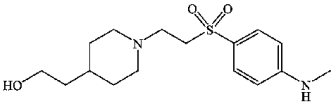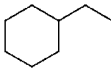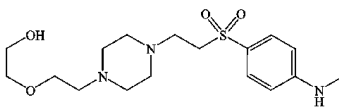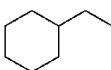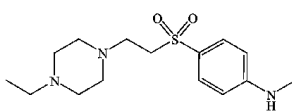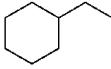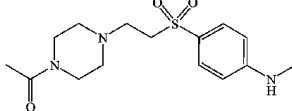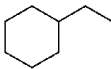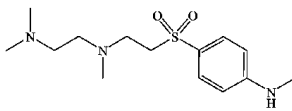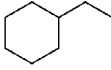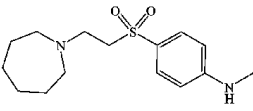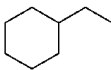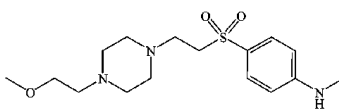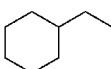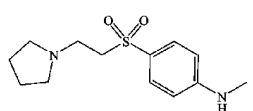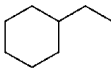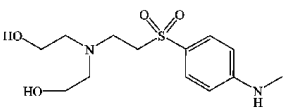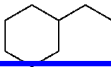
Compd	R1	R2	CDK2 inhibition (IC$_{50}$ (μM))	ΔE^{ONIOM}	ΔE^{ONIOM} (High A)	ΔE^{ONIOM} (Mid, AB-A)	ΔE^{ONIOM} (Low, ABC-AB)
58	(structure)	(structure)	0.16 ± 0.05	-23.40	-25.81	-3.81	6.22
59	(structure)	(structure)	0.12 ± 0.03	-12.87	-19.06	-0.18	6.37
60	(structure)	(structure)	0.34 ± 0.03	-11.91	-13.74	-4.77	6.60
61	(structure)	(structure)	0.54 ± 0.2	-11.55	-25.57	-0.01	14.03
62	(structure)	(structure)	0.45 ± 0.2	-19.29	-27.25	-4.30	12.26
63	(structure)	(structure)	0.45 ± 0.1	-24.52	-32.58	-0.20	8.26
64	(structure)	(structure)	0.045 ± 0.005	-14.59	-34.13	-0.06	19.60
65 (NU6271)	(structure)	(structure)	0.047 ± 0.001	-14.93	-25.30	0.03	10.33
66	(structure)	(structure)	0.023 ± 0.006	-29.15	-40.64	-0.42	11.91
67	(structure)	(structure)	3.7 ± 2.2	-19.04	-27.96	-0.31	9.23
68	(structure)	(structure)	0.078 ± 0.02	-30.94	-41.49	-0.01	10.56

Table 1. Continued

Compd	R1	R2	CDK2 inhibition (IC$_{50}$ (μM))	$\Delta E^{\mathrm{ONIOM}}$	$\Delta E^{\mathrm{ONIOM}}$ (High, A)	$\Delta E^{\mathrm{ONIOM}}$ (Mid, AB-A)	$\Delta E^{\mathrm{ONIOM}}$ (Low, ABC-AB)
69			0.34	-9.80	-21.35	-0.23	11.78
70			0.26	2.32	-21.26	-0.36	23.94
71			0.24	-20.15	-20.27	-0.07	0.19
72			0.31	-7.99	-17.77	-0.18	9.96
73			0.26	-19.07	-34.58	-0.55	16.07
74			0.23	-19.97	-33.37	-0.11	13.51
75			0.25	-18.39	-28.59	1.72	8.48
76			1.78	-8.30	-12.09	-0.15	3.94
77			0.29	-10.60	-24.81	-3.01	17.23
78			0.18	-22.13	-31.70	-5.02	14.59
79			0.11	-21.00	-35.17	-0.90	15.07
80		H—	13.0	-11.73	-14.47	-0.18	2.92
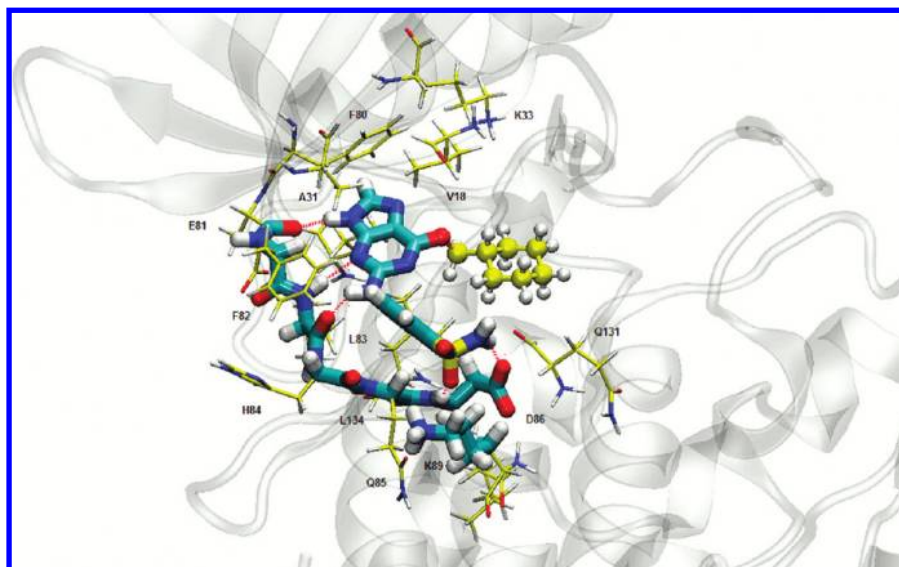
Figure 1. ONIOM3 partition scheme applied on inhibitor Nu6102 and CDK2 binding site model. The partition scheme was applied to all compounds with the calculation level setup as ONIOM (B3LYP/6-31G*: HF/3-21G: PM3) (see the main text for a detailed description).

this conformation of the CDK2 active site should be satisfied too by any other active compound.

It is important to take into account that due to the plasticity showed by kinases[34] some caution must be taken in the interpretation of the results when only one protein structure is used. Some recent studies on cross docking give important information about improved results when this aspect is taken into account.[35,36]

The entire set of compounds was built from the structure of compound **29** with the visualization program Insight II.[30] Then, they were submitted to an energy minimization and partial atomic charge determination as described above. After that, the docking protocol was applied, and the better conformers were chosen according to its docked free energy values and the position adopted in the CDK2 active site. The best conformers were used to perform hybrid calculations with ONIOM method.

ONIOM Calculations. The hybrid ONIOM method is implemented in Gaussian 03,[37] and it was developed by Morokuma and co-workers.[38−40] It enables different levels of theory to be applied to different parts of a molecule/system and combined to produce a consistent energy expression. The objective is to perform a high-level calculation on just a small part of the system and to include the effects of the remainder at lower levels of theory, with the end result being of similar accuracy to a high-level calculation on the full system. In our ONIOM model, the partition of the system was generated according to the three-layered ONIOM3 method. It was used to investigate the interactions between the set of inhibitors and the binding site of the T160pCDK2/cyclinA enzyme system.

In this work, we mainly focused on the study of the hydrogen bond interactions between hinge region and some residues at the solvent channel of CDK2 and different ligands with the purine scaffold. This goal was represented through the partition scheme used in our ONIOM calculations, where the ligand and its main hydrogen bond interactions within the active site were chosen to be part of the high level shell in the ONIOM calculation. As shown in Figure 1, for

the most active compound (**29**), the system was divided into three regions. The inner layer or the interaction region was treated at a high level of calculation (B3LYP/6-31G*). It is rendered in "licorice" sticks representation, and carbon atoms are colored in cyan. In this region were included the purine ring and the N2 substituent group of each inhibitor and the backbone atoms of residues Glu81 to Asp86 and the side chain of residues Lys89 and Asp86. The middle region was treated at the middle level of calculation (HF/3-21G). This part of the ONIOM system is sketched in ball and sticks representation with carbon atoms colored in yellow. In this region were only included the inhibitor substituent groups at position O6 of the purine ring. This part of the molecules was not included in the high level region because it was expected that its main contributions to the ligand binding were hydrophobic instead of electrostatic in nature. A recent work by Zhou et al.[41] showed that van der Waals energy contributions outweigh the electrostatic component in the CDK2 protein−ligand binding. The authors used in their study the same set of molecules reported by Gibson et al.[23] and which are part of the set of molecules used in our study to test the influence of O6 substituents groups in the protein−ligand binding.

The outer layer or the environmental region was treated at a lower level of calculation (PM3), and it included the remaining amino acids of the model system as it is shown in Figure 1. This region is rendered in thinner licorice sticks with carbon atoms colored in yellow. The previously described model was systematically applied to all compounds studied. The total ONIOM energy of the entire system was obtained from five independent energy calculations in ONIOM3

$$E^{ONIOM3}[ABC] = E[\text{High,A}] + E[\text{Mid, AB}] + \\ E[\text{Low, ABC}] - E[\text{Mid, A}] - E[\text{Low, AB}] \quad (1)$$

or according to the Gaussian03 output file

$$E^{ONIOM3}[ABC] = E_4 + E_5 + E_6 - E_2 - E_3 \quad (2)$$

STRUCTURAL BASIS OF GUANINE DERIVATIVES AS CDK2 INHIBITORS

J. Chem. Inf. Model., Vol. 49, No. 4, 2009 **895**

where energy E_4 corresponds to the interaction energy in the high model which was studied at the high level of calculation (in our case B3LYP/6-31G*). The H-bond interaction energy is defined as ΔE[High, A] + ΔE[Mid, AB].

To obtain the total ΔE^{ONIOM3} energy and the different delta energy contributions, it was necessary to calculate the ONIOM energies in the noninteracting system. This was accomplished by performing a single point energy calculation on the protein−ligand system separated by several Angstroms of distance each other.

Different energy contributions were obtained under the supermolecule approach.

The H-bond interaction energies were obtained for each protein−ligand complex as the arithmetic rest between the high and middle level energies (E(High, A) + ΔE(Mid, AB-A)) from the interacting protein−ligand and noninteracting protein−ligand systems.

Finally, the different energy values obtained were compared with the biological activity measured as IC_{50} values and previously reported in the literature. In general, those two steps in the computational protocol were performed very fast, with the prior partial atomic charges calculation on inhibitor being considered as the neck of the bottle for the docking process (almost 3 h depending on the size of the inhibitor). All ONIOM calculations were performed in a DELL computer with 8 Intel Xeon 1.60 GHz processors and 8GB RAM. Every ONIOM single point energy calculation was run in a single processor, and it took between 2 and $2^1/_2$ h.

RESULTS AND DISCUSSION

In Figure 2 is shown the alignment of the cocrystallized structure versus the docked structure for all inhibitors used to validate the docking methodology. The inhibitor structures corresponding to the X-ray crystal are entirely depicted in yellow, and those corresponding to the docked inhibitors are depicted as default (carbon atoms in cyan, oxygen atoms in red, nitrogen atoms in blue, and sulfur atoms in yellow). Both structures are sketched in "licorice" sticks representation. The carbon atoms belonging to the enzyme are rendered in cyan, and the most representative residues of the binding site in the protein structure are rendered as thinner sticks. The hydrogen bonds established between the inhibitors and the CDK2 hinge region are drawn as broken lines. As can be seen in Figure 2, the docked structures fitted in an optimal way with the inhibitor X-ray crystal structures. The purine ring was well located, near the hinge region (residues Glu81 to His84), to establish properly the typical hydrogen bond interactions described for this family of compounds. The O6-cyclohexylmethyl group showed the highest structure flexibility, and therefore its position with respect to the crystal structure was not always well fitted. The substituents at N2 position in the purine ring were well fitted by the docking program. It is noteworthy to mention the good fitting of the N2 substituent in compound **65**. Despite its high flexibility, the docked structure reproduced all the interactions reported previously for this substituent.[24]

In Table 2 are presented the values of the root mean standard deviation (rmsd) for the docked structures with respect to the cocrystal inhibitor structures. Recent studies compared various docking programs and algorithms devel-
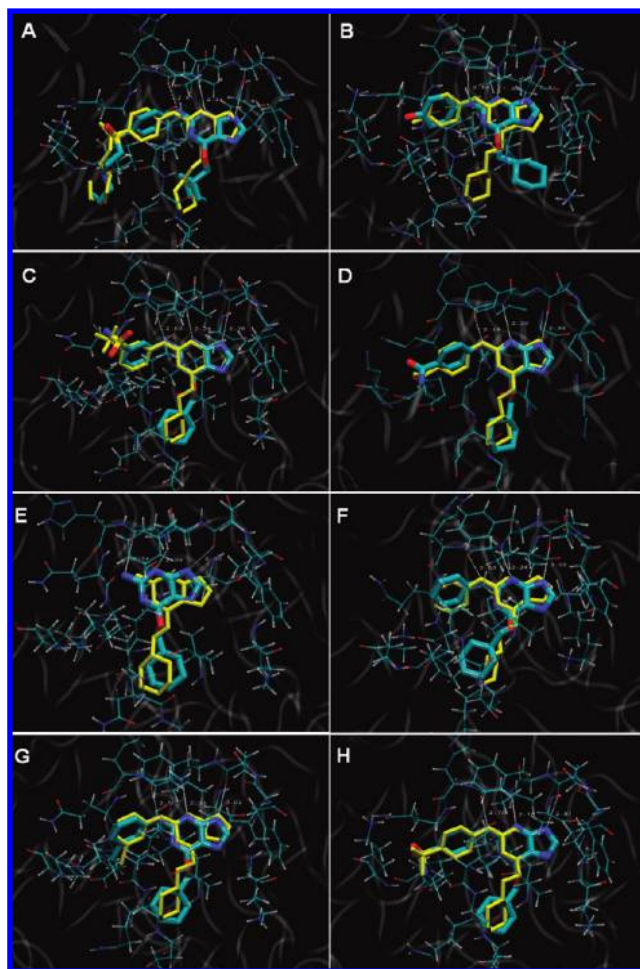
Figure 2. Alignment of inhibitor docked structures on inhibitor X-ray reference structures, for the most representative T160pCDK2/cyclin A complexes. The main residues within the CDK2 binding site are sketched in thin sticks. A. Compound **65** (PDB: 2G9X); B. Compound **40** (PDB: 1OI9); C. Compound **47** (PDB: 1OIU); D. Compound **48** (PDB: 1OIY); E. Compound **27** (PDB: 1H1P); F. Compound **28** (PDB: 1H1Q); G. Compound **34** (PDB: 1H1R); H. Compound **29** (PDB: 1H1S).

Table 2. Docking Accuracy[a]

PDB code of T160p-CDK2/cyclinA complex	cocrystallized inhibitor	rmsd (root mean squared deviation) values
2G9X	NU6271	1.42
1OI9	40	2.37
1OIU	47	1.09
1OIY	48	0.92
1H1P	NU2058	1.44
1H1Q	NU6094	1.28
1H1R	NU6086	1.02
1H1S	NU6102	1.00

[a] Root mean squared deviation (rmsd) values with respect to the reference crystal structure as a measure for the quality of the prediction.

oped to deal with the docking problem. It is proposed to focus on the rmsd value as a measure of the accuracy for the predicted docking poses.[42−44] A computed pose is considered "correct", if its rmsd value is <2.0 Å. Taking this in account, we can state that AutoDock3 found the correct binding mode of the ligands in seven of the eight cases analyzed.
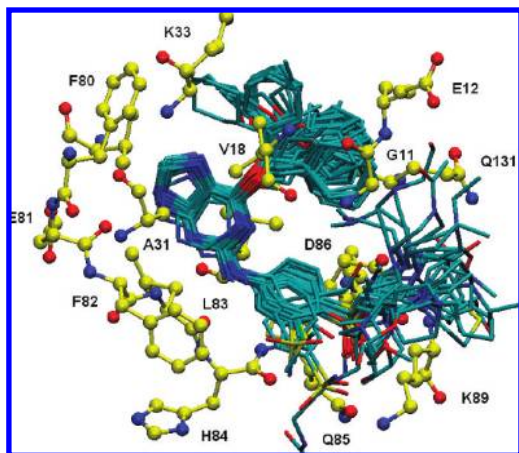
Figure 3. Alignment of all compound docked structures within the modeled CDK2 binding site. The main residues are identified with a one-letter representation.

In Figure 3 is shown the alignment of the docked structures for all compounds studied. The docking protocol was successful since almost all the ligands were docked into the CDK2 binding site and they fitted in the expected orientation. The purine ring was in the right position to establish the typical triplet of hydrogen bond interactions with the backbone structure of residues Glu81 and Leu83. NH-9 acts as a hydrogen bond donor to the backbone carbonyl group of Glu81 and N-3 and 2-NH₂ accept and donate a hydrogen bond to the backbone carbonyl and amide groups, respectively, of Leu83.[45] The purine's imidazole ring was oriented to make an edge-face aromatic—aromatic contact with the side chain of residue Phe80. In the O6-substituted guanine derivatives it is expected that O6-substituent groups are accommodated in the binding site for the ribose moiety of ATP and form highly complementary packing and hydrophobic interactions with an apolar pocket in the Gly-rich loop (residues 9—19).[46] In this sense, some structure—activity relationships for the O6-position have shown that a cyclic hydrophobic substituent such as cyclohexyl-methyl seems to be optimal.[23] In the present docking studies, it was observed that compounds with bulky and nonlinear O6-substituents adopted a correct pose within the CDK2 binding site. Some special and interesting cases were compounds **9** and **12**. These compounds have small and linear alkyl substituents (-CH₂C≡CH and -CH₂CH=CH₂). Their biological activities stand at the end of the activity spectrum studied here, and, therefore, their IC₅₀ values (90 ± 7 and 78 ± 13 μM, respectively) turn them into the less active compounds studied. The docked protocol did not find the typical guanine scaffold orientation for these two molecules within the CDK2 binding site, instead both of them were fitted at the bottom of the CDK2 binding site and they established some hydrogen bonds interactions with residues Glu51 and Lys33. Therefore, they were not included in the following hybrid ONIOM studies.

Finally, assuming a similar binding mode for compound **27**, substituents added to N2 position would project out of the ATP-binding cleft toward the solvent and contact the "specificity surface" of CDK2, with consequences for both potency and selectivity.[47] This was observed for the N2 guanine derivatives docked into the CDK2 binding site. In general, these substituents explored the specificity surface to a great extent, and they established some important

interactions with the residues located at the entrance of the CDK2 binding site. Of outstanding importance are the residues Asp86 and Lys89 with which the more potent inhibitors should establish the expected interactions. However, by simple visual inspection some other interactions were observed, for instance, some additional and new hydrogen bond interactions between the N2-substituents on the sulfonamide group with residues Glu8, Ile10, Glu12, Lys88, and Lys129. Those interactions were expected to lead inhibitors with enhanced selectivity for CDK2 as well as improved pharmaceutical properties; nevertheless the network of polar contacts formed by this kind of derivatives seems to be insufficient to compensate for the loss of more favorable interactions between CDK2 and the purine and aniline rings present in the more potent compounds.[24]

Overall, the docked inhibitors were fitted in the correct position within the CDK2 binding site, and they established all described interactions reported previously.

In order to compare the performance between ONIOM energies and scoring function energies given by AutoDock3, we plotted the AutoDock3 docked free energies against the log IC₅₀ values in an attempt to find a correlation model. A good correlation between these two variables was found, with a correlation coefficient $r = 0.79$ ($r^2 = 0.624$) (The linear regression equation and other relevant information derived from statistical analysis are presented in the Supporting Information.).

However the energy scores from docking studies did not make a clear distinction between the cluster of most active compounds and those in the middle range of potency (see the Supporting Information), and this is an important characteristic that needs to be satisfied by any promising score function. This important characteristic was accomplished by the H-bond interaction energies obtained with ONIOM protocol as is discussed below. In a further step, we proceed to apply the ONIOM method to each of the docked structures obtained with docking protocol.

In Table 1 are presented the total ΔE^{ONIOM3} energies and their components. In order to analyze in detail the importance of the previously defined subsystems on the total ONIOM binding energy, it was divided into three different contributions as follows:

$$\Delta E^{\text{ONIOM3}} = E(\text{interacting region}) - \\ [E(\text{interacting region + O6-substituent group}) + \\ E(\text{protein-ligand model})] \\ = \Delta E(\text{High, A}) + [\Delta E(\text{Mid, AB}) - \Delta E(\text{Mid, A})] + \\ [\Delta E(\text{Low, ABC}) - \Delta E(\text{Low, AB})] \\ = \Delta E(\text{High, A}) + \Delta\Delta E(\text{Mid, AB-A}) + \\ \Delta\Delta E(\text{Low, ABC-AB}) \quad (3)$$

Here $\Delta E(\text{High, A})$ is the interaction energy in the region A, namely the N2-substituted ligand-hinge region model interaction evaluated at the high level; $\Delta\Delta E(\text{Mid, AB-A})$ is the interaction energy between regions A and B (N2 and O6 substituted ligand-hinge region model) evaluated at the middle level; and $\Delta\Delta E(\text{Low, ABC-AB})$ is the interaction between regions AB and C evaluated at the low level, including the whole protein—ligand model complex. As shown in Table 1: for the most active ligand (**29**), the ONIOM3 (B3LYP/6-31G*: HF/3-21G: PM3) calculation gave $\Delta E(\text{High, A}) = -43.32$, $\Delta\Delta E(\text{Mid, AB-A}) = -0.29$, and $\Delta\Delta E(\text{Low, ABC-AB}) = 13.22$ kcal/mol. This means

STRUCTURAL BASIS OF GUANINE DERIVATIVES AS CDK2 INHIBITORS

J. Chem. Inf. Model., Vol. 49, No. 4, 2009 **897**

Figure 4. Plot of "H-bond interaction energy" (ΔE(High, A) + $\Delta\Delta E$(Mid, AB-A)) against biological activity represented as the log ($10^6/IC_{50}$) values.

that the total ligand-hinge model interaction, ΔE(High, A) + $\Delta\Delta E$(Mid, AB-A), was very favorable, and the interactions between the ligand and the remaining residues in the model, $\Delta\Delta E$(Low, ABC-AB), were to some extent repulsive and unfavorable. This general trend was observed for almost all inhibitors studied, except for the O6-substituted derivatives and some N2-alkyl derivatives, for which in some cases the $\Delta\Delta E$(Low, ABC-AB) energy was slightly repulsive or even favorable. This roughly means that bulky substituents at the N2 position in the purine ring destabilize the protein−ligand complex, but those unfav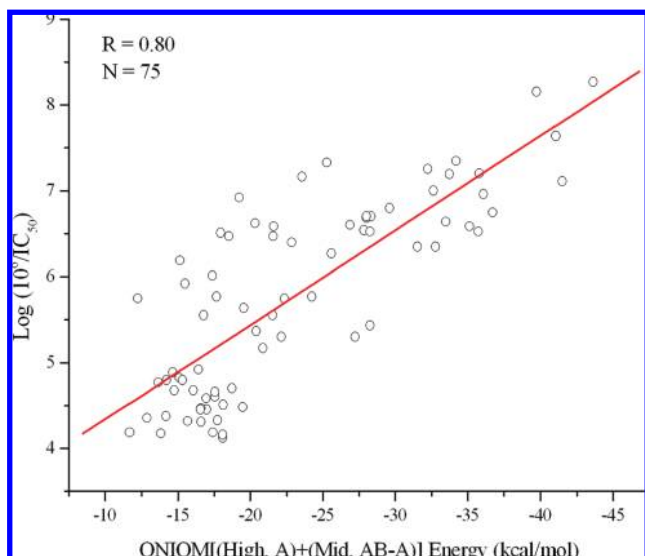orable interactions are compensated by the dominantly hydrogen bond interactions with the CDK2 hinge region and the "specificity surface" at the entrance of the binding site, especially with residues Lys89 and Asp86. Interestingly, the hydrogen bond interaction energy, represented in our model by ΔE(High, A) + $\Delta\Delta E$(Mid, AB-A), was the one that showed a better correlation (ΔE^{ONIOM3} showed a poor squared correlation coefficient value (r^2) = 0.033) with the biological activity, measured as IC_{50} values. The regression plot for the log of the experimental IC_{50} values versus the H-bond interaction energy shown in Figure 4 indicates that the predicted binding modes and estimated ONIOM H-bond energies are reliable, as is demonstrated in the following linear regression equation:

$$\log(10^6/IC_{50}) =$$
$$3.2401 - 0.11 \times ONIOM(\Delta E(\text{High, A}) +$$
$$\Delta\Delta E(\text{Mid, AB-A}))Energy(kcal/mol)$$
$$N = 75, r = 0.804, r^2 = 0.646, F_{(1.73)} = 133.03, p < 10^{-7}$$
$$(4)$$

where $\log(10^6/IC_{50})$ is the log of the experimental IC_{50} biological activity, ONIOM (ΔE(High, A) + $\Delta\Delta E$(Mid, AB-A)) is the estimated H-bond interaction energy as predicted by the ONIOM method, N is the number of compounds included in the model, r is the correlation coefficient, r^2 is the adjusted squared correlation coefficient, F is a testing factor of the reliability of the linear regression model, and p is the critical value for F at the specified degrees of freedom. A closer look to the statistical data derived from linear

regression shows a better performance for the ONIOM method compared with AutoDock3. Two quite separate pieces of information result from a regression analysis, one related to F-ratios and one to the r^2 value. High F-ratios lead us to conclude that two variables are related. High r^2 values, on the other hand, indicate that a large proportion of the variability has been explained. Those values are greater for the regression analysis performed from ONIOM energy data, which roughly means that this method can explain 64.6% of all variance and that there is good evidence that the two variables are related. However, it also provides some indication about whether other variables may be involved in determining the estimated value of log IC_{50} as is expected.

Regarding the poor correlation obtained from ONIOM total energy (ΔE^{ONIOM3}), it must be due to the static nature of the model used in this study. One should expect that allowing the model to relax during ONIOM calculations a more reliable correlation with log IC_{50} values will be obtained.

In the graph were included 75 of a total 80 compounds studied which nearly means that the present ONIOM hybrid model could explain the experimental activity of the compounds in an outstanding way. The five remaining compounds were not included in the correlation due to their interaction energy was many orders of magnitude higher (**46**, **52**, and **53**) or due to their different docked positions within the CDK2 binding site (**9** and **12**).

Furthermore, the relative ranking of the most potent and least potent compounds was identified, by capturing the subtleties in the substitution pattern on the O6 and N2 positions in the purine ring.

There are some theoretical and experimental data that support our findings about the importance of hydrogen bond interactions in this protein−ligand system. For instance, Aixiao et al.[48] found that residues Asp86, Leu83, Lys33, and Lys89 are important in determining the selectivity of compound 2PU by CDK2 or CDK4 enzymes. An energy decomposition analysis by residue showed that the electrostatic energy component is the most important determinant in the selectivity of 2PU by CDK4. Sun et al.[49] also determined the importance of the electrostatic energy component in the interactions of ATP within the CDK10 active site. Finally Jiang et al.[50] found a similar energy decomposition pattern in their study on the selectivity of compound NU6102 by CDK2/CDK4 enzymes. They also showed that Asp86 is a key residue that recognizes NU6102 more effectively with Cdk2 rather than Cdk4.

Other experimental findings support the crucial role of the hydrogen bonds in the hinge region as well as the role of the residues Asp86 and Lys89 in the improved selectivity showed by some CDK2 inhibitors.[24,45−47]

In a recent work Lyne et al.[51] reported the prediction of the relative potencies of members of a series of kinase inhibitors using molecular docking and MM-GBSA scoring. They included in their work a small set of CDK2 inhibitors (11 compounds) on which they performed molecular docking calculations with the program GLIDE.[52] After that, they estimated the ΔG of binding on the best docking poses using the MM-GBSA scoring approach.[53] They obtain a correlation model between the calculated binding energies and the pIC_{50} values with a correlation coefficient (r) = 0.71. In the present work, we have used a similar computational experiment in which the docking poses were generated with the software

package AutoDock3 and the binding energies for CDK2 inhibitors were computed within the ONIOM approach. It seems to be that our strategy is more advantageous due to the number of compounds tested and the quality of the correlation model. The time required to obtain the interaction energies must be improved with the aid of parallel computation. Resuming, the model showed a reasonable computational cost, and it could be systematized for a straightforward application to other groups of molecules with some medical or biological interest. However, we have found that some caution is necessary to have a high degree of confidence in the binding modes being used as input for the ONIOM protocol.

CONCLUSIONS

The molecular docking and hybrid ONIOM methods were used to obtain a statistically significant correlation model for the inhibition of CDK2 by a series of O6 and N2 substituted guanine derivatives. The molecular docking protocol used could predict in a proper way the orientation of the different ligands within the CDK2 binding site. The best ligand poses were used to perform hybrid quantum calculations within the ONIOM approach. It was found that, according to the energy data obtained from ONIOM calculations, the main energy contribution to the total interaction energy between the protein and the ligand in our model is given by the hydrogen bond interactions included in the high and middle levels (ΔE(High, A) + $\Delta\Delta E$(Mid, AB-A)). We observed that the interaction energy with the remaining amino acids in the active site is energetically unfavorable for inhibitors with bulky groups in the N2 position of the guanine ring. This is structurally important due to the fact that "specificity surface" has been considered as an important target in the design of new CDK2; nevertheless, our theoretical results and other experimental findings suggest that better characteristics in selectivity and potency cannot be attained targeting this region.

The interaction energy obtained from ONIOM protocol has two clear advantages: first it distinguished in a proper way the most active compounds from the nonactive ones, on the contrary to the docked energies from AutoDock3; and second, it allowed us to understand the most important contributions in this protein−ligand interaction, for instance, the H-bond interactions as it has been analyzed in this work.

In conclusion, we have combined two computational methods that allowed us to rationalize the main interactions between a group of guanine derivatives, used as CDK2 inhibitors, and a model of the CDK2 active site. We expect that, according with the accuracy and an improved performance of the computational protocol, these kinds of mixed computational protocols can help to clarify and speed up the search for new, potent and more selective CDK2 inhibitors.

ACKNOWLEDGMENT

Supporting Information Available: Plot of the AutoDock3 docked energy vs the log (10^6/IC$_{50}$) for the set of compounds studied (Figure SI1) and equation for statistical data from linear regression. This material is available free of charge via the Internet at http://pubs.acs.org.

REFERENCES AND NOTES

(1) Norbury, C.; Nurse, P. Animal-Cell Cycles and Their Control. *Annu. Rev. Biochem.* **1992**, *61*, 441–470.

(2) Morgan, D. O. Principles of CDK Regulation. *Nature (London)* **1995**, *374* (6518), 131–134.

(3) Hall, M.; Peters, G. Genetic alterations of cyclins, cyclin-dependent kinases and Cdk inhibitors in human cancer. *Adv. Cancer Res.* **1996**, *68*, 67–108.

(4) Sielecki, T. M.; Boylan, J. F.; Benfield, P. A.; Trainor, G. L. Cyclin-dependent kinase inhibitors: Useful targets in cell cycle regulation. *J. Med. Chem.* **2000**, *43* (1), 1–18.

(5) Watanabe, N.; Broome, M.; Hunter, T. Regulation of the Human WEE1HU CDK Tyrosine 15-Kinase during the Cell-Cycle. *EMBO J.* **1995**, *14* (9), 1878–1891.

(6) Coulonval, K.; Bockstaele, L.; Paternot, S.; Roger, P. P. Phosphorylations of cyclin-dependent kinase 2 revisited using two-dimensional gel electrophoresis. *J. Biol. Chem.* **2003**, *278* (52), 52052–52060.

(7) Pavletich, N. P. Mechanisms of cyclin-dependent kinase regulation: Structures of Cdks, their cyclin activators, and Cip and INK4 inhibitors. *J. Mol. Biol.* **1999**, *287* (5), 821–828.

(8) Losiewicz, M. D.; Carlson, B. A.; Kaur, G.; Sausville, E. A.; Worland, P. J. Potent Inhibition of CDC2 Kinase-Activity by the Flavonoid L86−8275. *Biochem. Biophys. Res. Commun.* **1994**, *201* (2), 589–595.

(9) Senderowicz, A. M.; Sausville, E. A. Preclinical and clinical development of cyclin-dependent kinase modulators. *J. Natl. Cancer Inst.* **2000**, *92* (5), 376–387.

(10) Hardcastle, I. R.; Golding, B. T.; Griffin, R. J. Designing inhibitors of cyclin-dependent kinases. *Annu. Rev. Pharmacol. Toxicol.* **2002**, *42*, 325–348.

(11) Knockaert, M.; Greengard, P.; Meijer, L. Pharmacological inhibitors of cyclin-dependent kinases. *Trends Pharmacol. Sci.* **2002**, *23* (9), 417–425.

(12) Toogood, P. L. Progress toward the development of agents to modulate the cell cycle. *Curr. Opin. Chem. Biol.* **2002**, *6* (4), 472–478.

(13) Shapiro, G. I. Preclinical and clinical development of the cyclin-dependent kinase inhibitor flavopiridol. *Clin. Cancer Res.* **2004**, *10*, 4270S–4275S.

(14) Vieth, M.; Higgs, R.; Robertson, D.; Shapiro, M.; Gragg, E.; Hemmerle, H. Kinomics-structural biology and chemogenomics of kinase inhibitors and targets. *Biochim. Biophys. Acta* **2004**, *1697* (1−2), 243–57.

(15) Fernandez, M.; Tudidor-Camba, A.; Caballero, J. Modeling of cyclin-dependent kinase inhibition by 1H-pyrazolo[3,4-d]pyrimidine derivatives using artificial neural network ensembles. *J. Chem. Inf. Model.* **2005**, *45* (6), 1884–1895.

(16) Gonzalez, M. P.; Caballero, J.; Morales Helguera, A.; Garriga, M.; Gonzalez, G.; Fernandez, M. 2D autocorrelation modelling of the inhibitory activity of cytokinin-derived cyclin-dependent kinase inhibitors. *Bull. Math. Biol.* **2006**, *68* (4), 735–751.

(17) Dureja, H.; Madan, A. K. Topochemical models for prediction of cyclin-dependent kinase 2 inhibitory activity of indole-2-ones. *J. Mol. Model.* **2005**, *11* (6), 525–531.

(18) Li, J. Z.; Liu, H. X.; Yao, X. J.; Liu, M. C.; Hu, Z. D.; Fan, B. T. Structure-activity relationship study of oxindole-based inhibitors of cyclin-dependent kinases based on least-squares support vector machines. *Anal. Chim. Acta* **2007**, *581* (2), 333–342.

(19) Samanta, S.; Debnath, B.; Basu, A.; Gayen, S.; Srikanth, K.; Jha, T. Exploring QSAR on 3-aminopyrazoles as antitumor agents for their inhibitory activity of CDK2/cyclin A. *Eur. J. Med. Chem.* **2006**, *41* (10), 1190–1195.

(20) Alzate-Morales, J. H.; Contreras, R.; Soriano, A.; Tunon, I.; Silla, E. A computational study of the protein-ligand interactions in CDK2 inhibitors: Using quantum mechanics/molecular mechanics interaction energy as a predictor of the biological activity. *Biophys. J.* **2007**, *92* (2), 430–439.

(21) Alzate-Morales, J. H.; Tiznado, W.; Santos, J. C.; Cardenas, C.; Contreras, R. Theoretical study on CDK2 inhibitors using a global softness obtained from the density of states. *J. Phys. Chem. B* **2007**, *111* (12), 3293–3297.

(22) Hardcastle, I.; Arris, C.; Bentley, J.; Boyle, F.; Chen, Y.; Curtin, N.; Endicott, J.; Gibson, A.; Golding, B.; Griffin, R.; Jewsbury, P.; Menyerol, J.; Mesguiche, V.; Newell, D.; Noble, M.; Pratt, D.; Wang, L.; Whitfield, H. N2-substituted O6-cyclohexylmethylguanine derivatives: potent inhibitors of cyclin-dependent kinases 1 and 2. *J. Med. Chem.* **2004**, *47* (15), 3710–3722.

STRUCTURAL BASIS OF GUANINE DERIVATIVES AS CDK2 INHIBITORS

J. Chem. Inf. Model., Vol. 49, No. 4, 2009 **899**

(23) Gibson, A.; Arris, C.; Bentley, J.; Boyle, F.; Curtin, N.; Davies, T.; Endicott, J.; Golding, B.; Grant, S.; Griffin, R.; Jewsbury, P.; Johnson, L.; Mesguiche, V.; Newell, D.; Noble, M.; Tucker, J.; Whitfield, H. Probing the ATP ribose-binding domain of cyclin-dependent kinases 1 and 2 with O(6)-substituted guanine derivatives. *J. Med. Chem.* **2002**, *45* (16), 3381–3393.

(24) Griffin, R.; Henderson, A.; Curtin, N.; Echalier, A.; Endicott, J.; Hardcastle, I.; Newell, D.; Noble, M.; Wang, L.; Golding, B. Searching for cyclin-dependent kinase inhibitors using a new variant of the cope elimination. *J. Am. Chem. Soc.* **2006**, *128* (18), 6012–6013.

(25) Morris, G. M.; Goodsell, D. S.; Halliday, R. S.; Huey, R.; Hart, W. E.; Belew, R. K.; Olson, A. J. Automated docking using a Lamarckian genetic algorithm and an empirical binding free energy function. *J. Comput. Chem.* **1998**, *19* (14), 1639–1662.

(26) Meng, E. C.; Gschwend, D. A.; Blaney, J. M.; Kuntz, I. D. Orientational Sampling and Rigid-Body Minimization in Molecular Docking. *Proteins* **1993**, *17* (3), 266–278.

(27) Blaney, J.; Dixon, J. A good ligand is hard to find: Automated docking methods. *Perspect. Drug Discovery Des.* **1993**, *1*, 301–319.

(28) Dewar, M. J. S.; Zoebisch, E. G.; Healy, E. F.; Stewart, J. J. P. Development and use of quantum mechanical molecular models. 76. AM1: a new general purpose quantum mechanical molecular model. *J. Am. Chem. Soc.* **1985**, *107*, 3902–3909.

(29) Stewart, J. J. P. *MOPAC, version 6*; Fujitsu Limited: Tokyo, Japan, 2006.

(30) *Insight II, version 2005*; Accelrys Inc.: San Diego, CA, 2005.

(31) Dauberosguthorpe, P.; Roberts, V. A.; Osguthorpe, D. J.; Wolff, J.; Genest, M.; Hagler, A. T. Structure and energetics of ligand-binding to proteins - *Escherichia-coli* dihydrofolate reductase trimethoprim, a drug-receptor system. *Proteins* **1988**, *4* (1), 31–47.

(32) Sanner, M. F. Python: A programming language for software integration and development. *J. Mol. Graphics Modell.* **1999**, *17* (1), 57–61.

(33) Berman, H.; Westbrook, J.; Feng, Z.; Gilliland, G.; Bhat, T.; Weissig, H.; Shindyalov, I.; Bourne, P. The Protein Data Bank. *Nucleic Acids Res.* **2000**, *28* (1), 235–242.

(34) Bartova, I.; Koca, J.; Otyepka, M. Functional flexibility of human cyclin-dependent kinase-2 and its evolutionary conservation. *Protein Sci.* **2008**, *17* (1), 22–33.

(35) Duca, J. S.; Madison, V. S.; Voigt, J. H. Cross-docking of inhibitors into CDK2 structures. 1. *J. Chem. Inf. Model.* **2008**, *48* (3), 659–668.

(36) May, A.; Zacharias, M. Protein-ligand docking accounting for receptor side chain and global flexibility in normal modes: Evaluation on kinase inhibitor cross docking. *J. Med. Chem.* **2008**, *51* (12), 3499–3506.

(37) Frisch, M. J.; Trucks, G. W.; Schlegel, H. B.; Scuseria, G. E.; Robb, M. A.; Cheeseman, J. R.; Montgomery, J. A., Jr.; Vreven, T.; Kudin, K. N.; Burant, J. C.; Millam, J. M.; Iyengar, S. S.; Tomasi, J.; Barone, V.; Mennucci, B.; Cossi, M.; Scalmani, G.; Rega, N.; Petersson, G. A.; Nakatsuji, H.; Hada, M.; Ehara, M.; Toyota, K.; Fukuda, R.; Hasegawa, J.; Ishida, M.; Nakajima, T.; Honda, Y.; Kitao, O.; Nakai, H.; Klene, M.; Li, X.; Knox, J. E.; Hratchian, H. P.; Cross, J. B.; Adamo, C.; Jaramillo, J.; Gomperts, R.; Stratmann, R. E.; Yazyev, O.; Austin, A. J.; Cammi, R.; Pomelli, C.; Ochterski, J. W.; Ayala, P. Y.; Morokuma, K.; Voth, G. A.; Salvador, P.; Dannenberg, J. J.; Zakrzewski, V. G.; Dapprich, S.; Daniels, A. D.; Strain, M. C.; Farkas, O.; Malick, D. K.; Rabuck, A. D.; Raghavachari, K.; Foresman, J. B.; Ortiz, J. V.; Cui, Q.; Baboul, A. G.; Clifford, S.; Cioslowski, J.; Stefanov, B. B.; Liu, G.; Liashenko, A.; Piskorz, P.; Komaromi, I.; Martin, R. L.; Fox, D. J.; Keith, T.; Al-Laham, M. A.; Peng, C. Y.; Nanayakkara, A.; Challacombe, M.; Gill, P. M. W.; Johnson, B.; Chen, W.; Wong, M. W.; Gonzalez, C.; Pople, J. A. *Gaussian 03, Revision A.1*; Gaussian, Inc.: Pittsburgh, PA, 2003.

(38) Svensson, M.; Humbel, S.; Froese, R. D.J.; Matsubara, T.; Sieber, S.; Morokuma, K. ONIOM: A multilayered integrated MO+MM method

(39) Dapprich, S.; Komaromi, I.; Byun, K. S.; Morokuma, K.; Frisch, M. J. A new ONIOM implementation in Gaussian98 Part I. The calculation of energies, gradients, vibrational frequencies and electric field derivatives. *J. Mol. Struct.: Theochem* **1999**, *462*, 1–21.

(40) Froese, R. D. J.; Morokuma, K. Hybrid methods. In *Encyclopedia of Computational Chemistry*; Schleyer, P.v. R., Ed.; John Wiley and Sons: Chichester, Sussex, 1998; Vol. 2, pp 1244−1257.

(41) Zhou, T.; Huang, D.; Caflisch, A. Is quantum mechanics necessary for predicting binding free energy. *J. Med. Chem.* **2008**, *51* (14), 4280–4288.

(42) Namasivayam, V.; Gunther, R. PSO@AUTODOCK: A fast flexible molecular docking program based on swarm intelligence. *Chem. Biol. Drug Des.* **2007**, *70* (6), 475–484.

(43) Kellenberger, E.; Rodrigo, J.; Muller, P.; Rognan, D. Comparative evaluation of eight docking tools for docking and virtual screening accuracy. *Proteins: Struct., Funct., Bioinf.* **2004**, *57* (2), 225–242.

(44) Warren, G. L.; Andrews, C. W.; Capelli, A. M.; Clarke, B.; LaLonde, J.; Lambert, M. H.; Lindvall, M.; Nevins, N.; Semus, S. F.; Senger, S.; Tedesco, G.; Wall, I. D.; Woolven, J. M.; Peishoff, C. E.; Head, M. S. A critical assessment of docking programs and scoring functions. *J. Med. Chem.* **2006**, *49* (20), 5912–5931.

(45) Arris, C. E.; Boyle, F. T.; Calvert, A. H.; Curtin, N. J.; Endicott, J. A.; Garman, E. F.; Gibson, A. E.; Golding, B. T.; Grant, S.; Griffin, R. J.; Jewsbury, P.; Johnson, L. N.; Lawrie, A. M.; Newell, D. R.; Noble, M. E. M.; Sausville, E. A.; Schultz, R.; Yu, W. Identification of novel purine and pyrimidine cyclin-dependent kinase inhibitors with distinct molecular interactions and tumor cell growth inhibition profiles. *J. Med. Chem.* **2000**, *43* (15), 2797–2804.

(46) Davies, T. G.; Bentley, J.; Arris, C. E.; Boyle, F. T.; Curtin, N. J.; Endicott, J. A.; Gibson, A. E.; Golding, B. T.; Griffin, R. J.; Hardcastle, I. R.; Jewsbury, P.; Johnson, L. N.; Mesguiche, V.; Newell, D. R.; Noble, M. E. M.; Tucker, J. A.; Wang, L.; Whitfield, H. J. Structure-based design of a potent purine-based cyclin-dependent kinase inhibitor. *Nat. Struct. Biol.* **2002**, *9* (10), 745–749.

(47) Davies, T. G.; Pratt, D. J.; Endicott, J. A.; Johnson, L. N.; Noble, M. E. Structure-based design of cyclin-dependent kinase inhibitors. *Pharmacol. Ther.* **2002**, *93*, 125–133.

(48) Aixiao, L.; Florent, B.; Francois, M.; Michel, D.; Baoshan, W. Interaction mode and selectivity of the 2PU inhibitor with the CDK4 and CDK2 cyclin-dependant kinases: A molecular dynamics study. *J. Mol. Struct.: Theochem* **2008**, *849* (1−3), 62–75.

(49) Sun, M.; Li, Z. S.; Zhang, Y.; Zheng, Q. C.; Sun, C. C. Homology modeling and docking study of cyclin-dependent kinase (CDK) 10. *Bioorg. Med. Chem. Lett.* **2005**, *15* (11), 2851–2856.

(50) Jiang, Y. J.; Zou, J. W.; Gui, C. S. Study of a ligand complexed with Cdk2/Cdk4 by computer simulation. *J. Mol. Model.* **2005**, *11* (6), 509–515.

(51) Lyne, P. D.; Lamb, M. L.; Saeh, J. C. Accurate prediction of the relative potencies of members of a series of kinase inhibitors using molecular docking and MM-GBSA scoring. *J. Med. Chem.* **2006**, *49* (16), 4805–4808.

(52) Friesner, R. A.; Banks, J. L.; Murphy, R. B.; Halgren, T. A.; Klicic, J. J.; Mainz, D. T.; Repasky, M. P.; Knoll, E. H.; Shelley, M.; Perry, J. K.; Shaw, D. E.; Francis, P.; Shenkin, P. S. Glide: A new approach for rapid, accurate docking and scoring. 1. Method and assessment of docking accuracy. *J. Med. Chem.* **2004**, *47* (7), 1739–1749.

(53) Huang, N.; Kalyanaraman, C.; Irwin, J. J.; Jacobson, M. P. Physics-based scoring of protein-ligand complexes: Enrichment of known inhibitors in large-scale virtual screening. *J. Chem. Inf. Model.* **2006**, *46*, 243–253.